

Daily gridded meteorological variables in Brazil (1980–2013)

Alexandre C. Xavier,^a Carey W. King^{b*} and Bridget R. Scanlon^c

^a Department of Rural Engineering, Federal University of Espírito Santo, Vitória, Brazil

^b Energy Institute, The University of Texas at Austin, TX, USA

^c Bureau of Economic Geology, The Jackson School of Geosciences, The University of Texas at Austin, TX, USA

ABSTRACT: Basic meteorological data are essential for evaluating impacts of spatiotemporal variability in climate forcing on hydrology and agroecosystems. The objective of this work was to develop high-resolution grids ($0.25^\circ \times 0.25^\circ$) of daily precipitation, evapotranspiration, and the five climate variables generally required to estimate evapotranspiration for Brazil. These five variables are maximum and minimum temperature, solar radiation, relative humidity, and wind speed. We tested six different interpolation schemes to create the grids for these variables. The data were obtained from 3625 rain gauge and 735 weather stations for period of 1980–2013. We used a cross-validation approach that compares point observed data to point interpolated estimates to select the best interpolation scheme for each climate variable. We also present the performance of the best interpolation for each climate variable at daily timescales and for river basins. The inverse distance weighting and angular distance weighting methods produced the best results. Performance of all methods was poorer prior to 1995 because of fewer stations and available data. The performance of the interpolation varies for different seasons for almost all variables. Forecasting capability was tested for precipitation only and performed adequately for the system state (wet or dry). Variations in the interpolation schemes across river basins are primarily attributed to differences in gauge or station network density. This freely available gridded meteorological data set significantly advances the availability of climate data in Brazil.

KEY WORDS Brazil; interpolation; precipitation; evapotranspiration; meteorological variables; data set; gridded data

Received 21 March 2015; Revised 22 August 2015; Accepted 1 September 2015

1. Introduction

It is becoming increasingly important to have available and reliable meteorological data to understand trends in climate variables and climate extremes, as well as their impacts on water resources and agriculture (Jones *et al.*, 2003; Steduto *et al.*, 2009). The two dominant components of water budgets in most regions are precipitation and evapotranspiration (ET). There are a variety of global products available for precipitation and ET. For example, global precipitation products based solely on satellite data include the US National Oceanic and Atmospheric Administration (NOAA) Climate Prediction Center (CPC) Morphing Technique (CMORPH) and the Tropical Rainfall Measuring Mission (TRMM) with daily precipitation data since 1998 at a spatial resolution of $0.25^\circ \times 0.25^\circ$ (Huffman *et al.*, 2007). Other products based solely on ground-based station data include those from the NOAA Global Precipitation Climatology Centre (GPCC) and the East Anglia University Climatic Research Unit (CRU). Some meteorological and climate products combine satellite and ground-based data. The Global Precipitation Climatology Project (GPCP) is one such product with daily precipitation data at 1° of resolution from 1996 to present (Huffman *et al.*, 2001).

The US PRISM (Parameter-elevation Regressions on Independent Slopes Model) incorporates point data, a digital elevation model, and other information to provide digital grid estimates of daily, monthly, and annual precipitation (Daly *et al.*, 2008). There are also a number of global satellite-based ET products, including MOD16 based on MODIS (Moderate Resolution Imaging Spectroradiometer) satellite data (Mu *et al.*, 2011), NOAA AVHRR (Advanced Very High Resolution Radiometer) product (Zhang *et al.*, 2010) and others using ground-based eddy covariance station data (FLUXNET) (Jung *et al.*, 2009), and a gridded monthly data set generated from meteorological stations by CRU (Harris *et al.*, 2014). Global land surface models also include precipitation forcing data and simulated ET products (Global Land Data Assimilation System, Rodell *et al.*, 2004). While these products are available at variable spatial and temporal resolutions, it is important to compare satellite and model-based products with station data. For example, GPCP and TRMM measurements generally require validation, and this validation is performed by comparing to ground-based rain gauges (Karaseva *et al.*, 2012; Li *et al.*, 2012). Thus, ground-based station records provide a fundamental building block on which to evaluate other meteorological products.

The objective of this study was to develop a gridded data set of precipitation and reference ET (ET_o) based on the most comprehensive ground-based station data available

* Correspondence to: C. W. King, Energy Institute, The University of Texas at Austin, 2304 Whitis Ave, Stop C2400, Austin, TX 78712-1781, USA. E-mail: careyking@mail.utexas.edu

for Brazil. Because many applications of meteorological data require a uniform gridded data set (e.g. to compare with satellite observations or climate model calculations), it is important to process ground-based station data to develop such a product. We present the data at 0.25° (approximately 28 km at the equator) spatial resolution and at both daily and monthly temporal resolutions. In order to compare the interpolation methods used to estimate values for each grid cell, we used a cross-validation procedure that compares point observed data to point interpolated estimates. That is to say, while our goal is to produce a value for a grid cell that inherently provides a metric of a given meteorological variable (e.g. precipitation) that is assumed to be representative of the entire grid cell, our only procedure for assessing accuracy of our interpolation methods is to compare a point interpolation estimate to a point measurement (Haylock *et al.* (2008) also discuss this concept).

The main sources of weather data are those measured directly from rain gauges and weather stations. In Brazil, there are large areas without any rain gauges or weather stations. Furthermore, the data quality is sometimes poor with a large number of missing data. However, these are common problems for creating gridded data sets. One existing product, for precipitation only, is a daily gridded (1° and 2.5°) data set from Earth System Research Laboratory (http://www.esrl.noaa.gov/psd/data/gridded/data.south_america_precip.html) for South America using rain gauge data for 1940–2012 (Liebmann and Allured, 2005). The ESRL (Earth System Research Laboratory) gridded data sets include large areas of missing values, because they do not include interpolation beyond the local area of each grid point. This contrasts with the added value of interpolation in the new gridded product.

Many projections indicate that Brazil may be one of the few areas where food production can be substantially increased to meet rising global food demand (Bruinsma, 2003). In 2012 for worldwide crop production, Brazil ranked first globally in production of sugar cane, green coffee, and oranges; second in production of soybeans, dry beans, and papaya; and third in production of maize (FAOSTAT, 2014). In addition, Brazil is a model area for biofuel production using sugarcane which has also been expanding in the past decade (ICONE, 2012). Calculating the water footprint of agriculture requires basic meteorological parameters, such as precipitation and reference evapotranspiration (ET_o). Developing a reliable meteorological product helps in addressing whether ET in existing and expanding agricultural regions exceeds precipitation. Thus, we then have requisite data to understand water demand *versus* availability in regions across Brazil, and to assess the need and availability of water for irrigation, municipal supply, and other demands.

The organization of this article is as follows. Section 2 describes data sources, equations used to calculate ET_o, and interpolation methods for creating the gridded data. Section 3 then compares each of the interpolation methods for each meteorological variable using several statistical measurements for comparison. We selected the

Table 1. Total number of rain gauges collected per basin and source.

Basin name	INMET Conventional	INMET Automatic	ANA	DAEE	Total
Amazon river	33	61	446	0	540
Tocantins river	18	42	179	0	239
North Atlantic region	57	78	311	0	446
Sao Francisco river	41	43	322	0	406
Central Atlantic region	40	78	393	31	542
Parana river	49	120	466	386	1021
Uruguay river	11	25	154	0	190
South Atlantic region	11	28	165	37	241
Total	260	475	2436	454	3625

best interpolation method for each variable over the entire time span of our data.

2. Data and methods

2.1. Data sources

Generally, the required variables to calculate ET_o are maximum and minimum temperature (T_{\max} and T_{\min}), solar radiation (R_s), wind speed at 2 m height (u_2), and relative humidity (RH). Individually, some of these variables can be used to estimate crop productivity (Tao *et al.*, 2014).

Our data set includes daily observed data collected from rain gauges as well as conventional and automatic weather stations from the period of 1 January 1980 to 31 December 2013. The meteorological data types are maximum temperature (T_{\max} , °C), minimum temperature (T_{\min} , °C), mean RH (%), wind speed at 2 m height (u_2 , m s⁻¹), precipitation (pr, mm), and either the daily duration of sunshine (n , hours) from conventional weather stations or daily solar radiation (R_s , MJ m⁻²) from automatic stations. We also include two indicators of the quality of each grid cell: the number of included stations with data, and the geodesic distance of the nearest reporting station with data.

The sources of the data are the ‘Instituto Nacional de Meteorologia’ (INMET), the ‘Agência Nacional de Águas’ (ANA), and ‘Departamento de Águas e Energia Elétrica de São Paulo’ (DAEE). Table 1 shows the number of weather stations per major water basin in Brazil. INMET data are from weather stations that collect all of the aforementioned weather variables. The data from ANA and DAEE are limited to precipitation pr. ANA provides the major source of pr data via 2436 rain gauge stations (67% of all the rain gauges). We checked if there were any duplicate rain gauge or weather station data provided by more than one agency. We observed six pairs of rain gauges with the same coordinates, but in each case, the data were not duplicated. We did not observe any weather station data with duplicate coordinates. Thus, we did not remove any rain gauge or weather station data from our data set.

Table 2. Tests applied on the observed data to validate them.

Variable	Test	References	Number of data points removed
pr (mm)	$0 \leq \text{pr} < 450$	Liebmann and Allured (2005)	92
T_{\max}, T_{\min} (°C)	$-30 \leq T_{\max}, T_{\min} < 50$	Shafer <i>et al.</i> (2000)	0
RH (%)	$0 \leq \text{RH} < 100$		0
R_s (MJ m^{-2})	$0.03R_a \leq R_s < R_a$	Moradi (2009)	70
u_2 (m s^{-1})	$0 \leq u < 100$	Shafer <i>et al.</i> (2000)	0

2.1.1. Data quality and homogeneity

We performed a simple quality control check for the raw data by discarding all data that failed any of the screening tests listed in Table 2. For example, for pr, 94 of the approximately 32 million days with observed data have values exceeding 450 mm. Because the targeted use of our gridded data is for crop ET and growth analysis, our main goal is to remove ‘obvious’ outliers, or extreme values. A more complete analysis would require confirmation of the discarded data per Table 2 to confirm whether the data are valid. While there could be worthwhile benefits to assess all of our discarded data, it is beyond the scope of this work (Wijngaard *et al.*, 2003; You *et al.*, 2007).

We also applied a qualitative test for homogeneity of each type of data, except for the precipitation data. We did not apply an objective quantitative test for homogeneity of the data, but instead used only a simple visual comparison of data with those from surrounding stations. Several methodologies for analysis of homogeneity are described in Peterson *et al.* (1998), where one of the primary tools is checking historical metadata files, but the metadata are not available to us for this study.

Application of an objective homogeneity test requires construction of a reference against which to test the candidate station. As mentioned previously, Brazil has a low density of weather stations in most areas, and several stations have a great number of missing data. Difficulties in testing homogeneity for South America data are discussed in Haylock *et al.* (2006) for daily precipitation. Haylock *et al.* (2006) did not perform statistical homogeneity tests due to a lack of nearby surrounding stations and interannual variability in precipitation due to El Niño Southern Oscillation. Vincent *et al.* (2005) tested the homogeneity of 68 stations with maximum and minimum daily temperature data where 19 and 22 stations, respectively, presented potential inhomogeneity. However, they did not remove the potentially inhomogeneous data because of the limited data availability. Therefore, for our data set, we did not perform homogeneity analysis for pr.

For the variables T_{\max} , T_{\min} , R_s , RH, and u_2 , we performed a visual homogeneity check. This visual homogeneity test plots the time series of data from the candidate station along with the average of data from several surrounding stations. This average approximates data as if from a validated reference station. The number of surrounding stations was selected such that we had at least five surrounding data to calculate the average. For example, if we are checking homogeneity of T_{\max} , and the

five nearest surrounding weather stations have no missing data, then we only need to use these five stations. However, if for 1 day only two of the stations have observed T_{\max} , the next three closest stations with observed T_{\max} on that day must be selected. In general, less than 20 weather stations were used to calculate an average time series for our homogeneity test for any candidate station.

When we observed a clear inhomogeneity in trend in some part of the time series of the candidate station, we removed those data. In Figure 1, we show examples of data that were removed, and Table 3 indicates the number of stations with inhomogeneous data and the quantity of data removed. The variables T_{\min} and u_2 have more days with inhomogeneous data, although they are few compared to the total amount of data (for each variable, <0.4% of the raw data were removed). We can only speculate on the causes of the inhomogeneities. For example, in Figure 1(a), (b), and (d) (T_{\max} , RH, and u_2), the instruments seem to be temporally defective, while Figure 1(c) (R_s) indicates that the problem could be the temporary use of different units. This type of units problem could be fixed if we had access to the station metadata.

2.2. Reference ET

We calculated daily reference ET using the Food and Agriculture Organization of the United Nations (FAO) Penman–Monteith method (ET_o, Allen *et al.* (1998); Raes (2012)) shown in Equation (1) for both the conventional and automatic weather stations. The variables used to calculate ET_o are the observed daily T_{\max} , T_{\min} , RH, u_2 , and R_s or n . We calculated ET_o at weather stations only for days in which all required data are available and remain after the screening process per Table 2. For example, if for 1 day and station all variables are present except for u_2 , then we did not calculate ET_o.

$$\text{ET}_o = \frac{0.408\Delta (R_n - G) + \gamma \frac{900}{T+273} u_2 (e_s - e_a)}{\Delta + \gamma (1 + 0.34u_2)} \quad (1)$$

In Equation (1), ET_o is reference ET (mm day^{-1}), R_n is net radiation ($\text{MJ m}^{-2} \text{day}^{-1}$), G is soil heat flux density ($\text{MJ m}^{-2} \text{day}^{-1}$), T is air temperature at 2 m height (°C), u_2 is wind speed at 2 m height (m s^{-1}), e_s is saturation vapour pressure (kPa), e_a is actual vapour pressure (kPa), $e_s - e_a$ is the saturation vapour pressure deficit (kPa), Δ is the slope vapour pressure curve ($\text{kPa } ^\circ\text{C}^{-1}$), and γ is the psychrometric constant ($\text{kPa } ^\circ\text{C}^{-1}$).

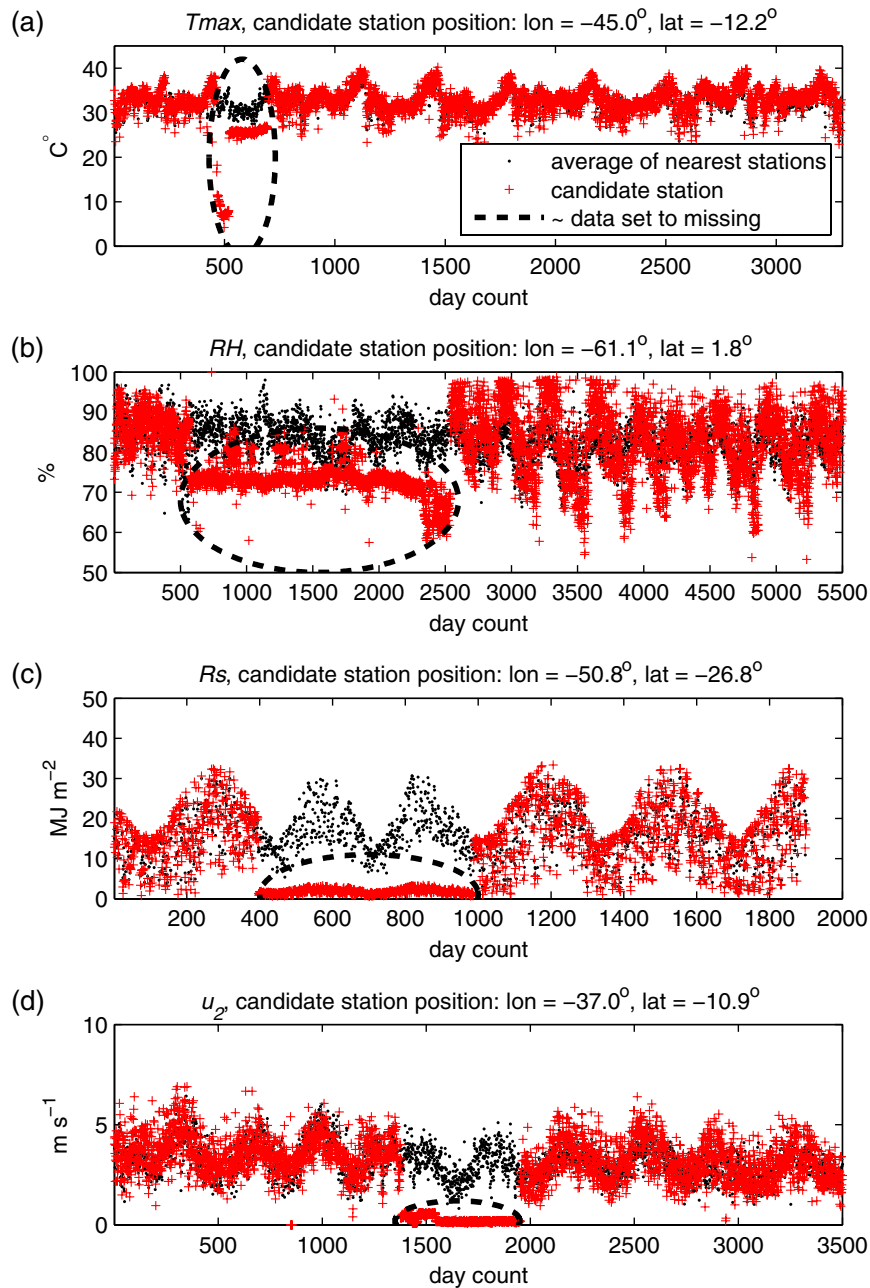


Figure 1. Examples of using a visual analysis method for testing homogeneity of data time series. The red dots indicate data from the candidate station. The black dots indicate the arithmetic average of the nearest surrounding stations. Any data that visually fall outside of the average range and average trend were removed as indicated by the dashed ovals.

Table 3. A summary of the homogeneity check showing that we discarded less than 0.4% of data for each variable required to estimate ET_o.

Variable	Number of stations with homogeneity problem	Number of data points removed	% of total data removed
T_{\max}	3	1186	0.02
T_{\min}	13	21 108	0.36
R_s	24	8484	0.14
RH	5	2116	0.03
u_2	7	12 008	0.20

In our case, G was considered zero; T was the average of T_{\max} and T_{\min} ; e_a was estimated with the aid of RH, T_{\max} , and T_{\min} as follows:

$$e_a = \frac{\text{RH}}{100} \left(\frac{e^\circ(T_{\max}) + e^\circ(T_{\min})}{2} \right) \quad (2)$$

where $e^\circ(T_{\max})$ and $e^\circ(T_{\min})$ are saturation vapour pressure at the air maximum and minimum temperatures, respectively. R_n was calculated as follows:

$$R_n = R_{\text{ns}} - R_{\text{nl}} \quad (3)$$

where R_{ns} is incoming net shortwave radiation that is a function of albedo (assumed as 0.23 for hypothetical grass reference crop), and R_{nl} is the outgoing net longwave radiation that is a function of T_{max} , T_{min} , e_a , R_s , and R_{so} , where R_{so} is clear-sky radiation ($\text{MJ m}^{-2} \text{day}^{-1}$) that is calculated. R_s is directly measured in the automatic weather stations. For the conventional weather stations, R_s is estimated with the aid of n , the maximum possible duration of sunshine (N , hour), and the extraterrestrial radiation (R_a , $\text{MJ m}^{-2} \text{day}^{-1}$) as:

$$R_s = \left(0.25 + 0.50 \frac{n}{N}\right) R_a \quad (4)$$

where R_a and N are calculated as in Allen *et al.* (1998).

2.3. Interpolation methods

Developing a gridded meteorological product from station data is challenging because stations represent points with varying densities in a region, stations come online at different times, and many stations have periods of missing records. A variety of approaches have been developed to interpolate station data, and we compare these methods for each of our weather variables.

We tested six interpolation methodologies and selected the best one for precipitation and each variable needed to estimate ETo: (1) average inside the area of $0.25^\circ \times 0.25^\circ$ (AVERAGE), (2) natural interpolation (NATURAL), (3) thin plate spline (THINPLATE), (4) inverse distance weighting (IDW), (5) angular distance weighting (ADW), and (6) ordinary point kriging (OPK). During cross-validation analysis for each of the interpolation methods, we used the five nearest available stations with data in the neighbourhood of the query position. For comparison, New *et al.* (2000) used eight nearest stations in monthly interpolation of weather data. When the query position was outside the convex hull (e.g. on the border of Brazil), the nearest data were used. We did not use elevation data as input for interpolation.

For all variables except pr, within each $0.25^\circ \times 0.25^\circ$ grid square, we considered the centroid as the single interpolation location. For pr, we used a different approach because of the higher density of precipitation data (e.g. there are often many observed data within each grid square). Because of the higher density of precipitation gauges, we calculated a single value for a grid point from the average of 25 individual interpolations within that grid taken at 0.05° spacing, similar to the approach used in Haylock *et al.* (2008).

2.3.1. Arithmetic average

We calculated the arithmetic average (AVERAGE) equal to the sum of the data divided by the number of data. For each $0.25^\circ \times 0.25^\circ$ grid square, we considered the centroid as the interpolation location and included a maximum of five nearest data. Our approach differs from that used by Liebmann and Allured (2005) for the South American gridded precipitation product. They used the average in a corresponding geographic ellipse, with no explicit limit on

the number of stations, and while Liebmann and Allured (2005) did not assign any value to grid cells that did not have any station data, we assigned a data point that was nearest to the centroid, but lies outside, the grid cell of interest.

2.3.2. Thin plate spline

The THINPLATE is a common interpolation technique used for weather data (Xia *et al.*, 2001; Wu *et al.*, 2014), particularly for regions with sparse station data (New *et al.*, 2002). Our calculations were performed in Matlab using the internal function *TPAPS*.

2.3.3. Natural neighbour

We included natural neighbour interpolation (NATURAL) as part of the normal suite of methods (Sibson, 1981; Hofstra *et al.*, 2008). NATURAL uses Thiessen polygons and triangulation to select which nearby data points to use, while weighting each of them based upon its associated area. The interpolation surface is constructed to reproduce the observation data at the surrounding weather stations. Our calculations were performed in Matlab using the internal function *GRIDDATA* with the 'natural' method.

2.3.4. Inverse distance weighting

In the IDW method, the interpolated quantity at a location is based upon a weighting (Equation (5), W_k) that is inversely proportional to the distance between the point and the data from the k th nearby weather station.

$$W_k = \frac{1}{d_k^p} \quad (5)$$

Here, d is the geodesic distance of station k and the specified point, and p is the power parameter that we set equal to 2, as suggested by Ly *et al.* (2011). The number of weather stations to consider for interpolating at a chosen point were the nearest five, selected after cross validation.

2.3.5. Angular distance weighting

In the ADW method, the weighting for the data from the surrounding stations is calculated using both the distance and the angles (or orientation) between weather stations. The distance weight is calculated using a correlation decay function with the empirically derived correlation decay distance (CDD) (see Equation (6)).

$$r = e^{-x/\text{CDD}} \quad (6)$$

In Equation (6), x is the distance from the gridded point of interest and a nearby weather station. For each station, we calculated the correlation (r) with all other stations. Then, we solved for the CDD that minimizes the least squares error between the values of r_k corresponding to the x_k calculated using observed data and $r(x)$ using Equation (6). On average, our CDD values are around 200 km for pr (similar to those of Hofstra and New (2009), Europe) and 800 km for the other weather variables (similar to

those of New *et al.* (2000), temperature global). The distance weighting for each station (k) is calculated using Equation (7):

$$w_k = r^m \tag{7}$$

where we selected the exponent m for each meteorological variable during cross validation (see Section 2.4), testing for each variable the integer values 1–8. We selected the following exponents: $m = 1$ for pr and u_2 ; $m = 6$ for ETo, T_{\max} , and R_s ; and $m = 4$ for T_{\min} and RH.

The second part of the distance weight is the angular weight (a_k , Equation (8)) for each of the $n_j = 5$ (for our study) selected stations used for interpolation:

$$a_k = \frac{\sum_{l=1}^{n_j} w_l (1 - \cos \theta_j(k, l))}{\sum_{l=1}^{n_j} w_l}, \quad l \neq k \tag{8}$$

where $\theta_j(k, l)$ is the angle formed by stations l and k with the vertex at the interpolating point of interest. To weight the values of the surrounding stations for interpolating at the point of interest, the distance and angle weightings are combined for each k^{th} station (W_k):

$$W_k = w_k (1 + a_k) \tag{9}$$

2.3.6. Ordinary point kriging

The OPK methodology has an expected average error of zero. To weight the spatial dependency of the observed data, OPK uses the variogram estimator (Webster and Oliver, 2007). We used monthly variogram estimators as the average of the daily semivariances for each month. During our cross-validation process for comparing interpolation methods, we decided to use the spherical model to model the semivariance.

2.4. Cross validation

We used a cross-validation procedure for comparing the accuracy of the interpolation methods. The process is as follows. For each observed data point at a test weather station (i.e. for each observed variable at each station and each day), we ‘remove’ it from the data set. We then use each of the interpolation methods to estimate the weather variable at this test station. This procedure is similar to that used by Daly *et al.* (2008) and Hofstra *et al.* (2008). For precipitation, for example, we have approximately 32 million observed daily data. Thus, the total number of cross-validation calculations was approximately 192 million (32 million of data times six interpolation methods).

We used the following statistics to compare the accuracy of the observed data (X) with our interpolated estimates (Y): the coefficient of correlation (R), the bias, the root mean square error (RMSE), the mean absolute error (MAE), the compound relative error (CRE), the critical

success index (CSI), and the percent correct (PC).

$$R = \frac{\sum_{i=1}^n (X_i - \bar{X})(Y_i - \bar{Y})}{\sum_{i=1}^n \sqrt{(X_i - \bar{X})^2} \sqrt{(Y_i - \bar{Y})^2}} \tag{10}$$

$$\text{Bias} = \bar{Y} - \bar{X} \tag{11}$$

$$\text{RMSE} = \sqrt{\frac{\sum_{i=1}^n (X_i - Y_i)^2}{n}} \tag{12}$$

$$\text{MAE} = \frac{1}{n} \sum_{i=1}^n |X_i - Y_i| \tag{13}$$

$$\text{CRE} = \frac{\sum_{i=1}^n (X_i - Y_i)^2}{\sum_{i=1}^n (X_i - \bar{X})^2} \tag{14}$$

$$\text{CSI} = \frac{a}{a + b + c} \tag{15}$$

$$\text{PC} = \frac{a + d}{a + b + c + d} \tag{16}$$

In Equations 10–16, \bar{X} and \bar{Y} are the mean of X and Y , and n is the number of observed data available. CSI and PC are forecast quality measurements where a is number of hits (correct forecast), b is number of false alarms (event was forecast but not observed), c is number of missed forecasts (event occurred but was not forecast), and d is number of correct rejections (event did not occur and was not forecast) (Hofstra *et al.*, 2008; Wilks, 2011).

CRE and R are measurements of similarity, where CRE is zero when X equals Y . R measures the degree of linear dependence of the variables, varying from -1 to 1 . Bias indicates whether the interpolated estimates tend to be lower or higher than the observed data (a bias of zero is ideal). RMSE and MAE measure accuracy, such that when observed and estimated data are similar, RMSE and MAE are close to zero, indicating a more accurate interpolation. RMSE calculates the square of deviation between observed and estimated values, and is thus more sensitive to larger errors. Bias, RMSE, and MAE have the same units as the variable.

PC was calculated only for pr to verify whether the interpolated methods were able to forecast the state of pr. The state of pr was defined as ‘wet’ or ‘dry’, where a wet state is defined as $\text{pr} > 0.5 \text{ mm day}^{-1}$, and dry otherwise. With CSI, we test whether the interpolation methods are able to forecast extreme values. Extreme values are those that fall below the 5th (CSI low, CSIL) percentile or above the 95th percentile (CSI high, CSIH) in the observed and estimated data (see Hofstra *et al.* (2008)). Because of a

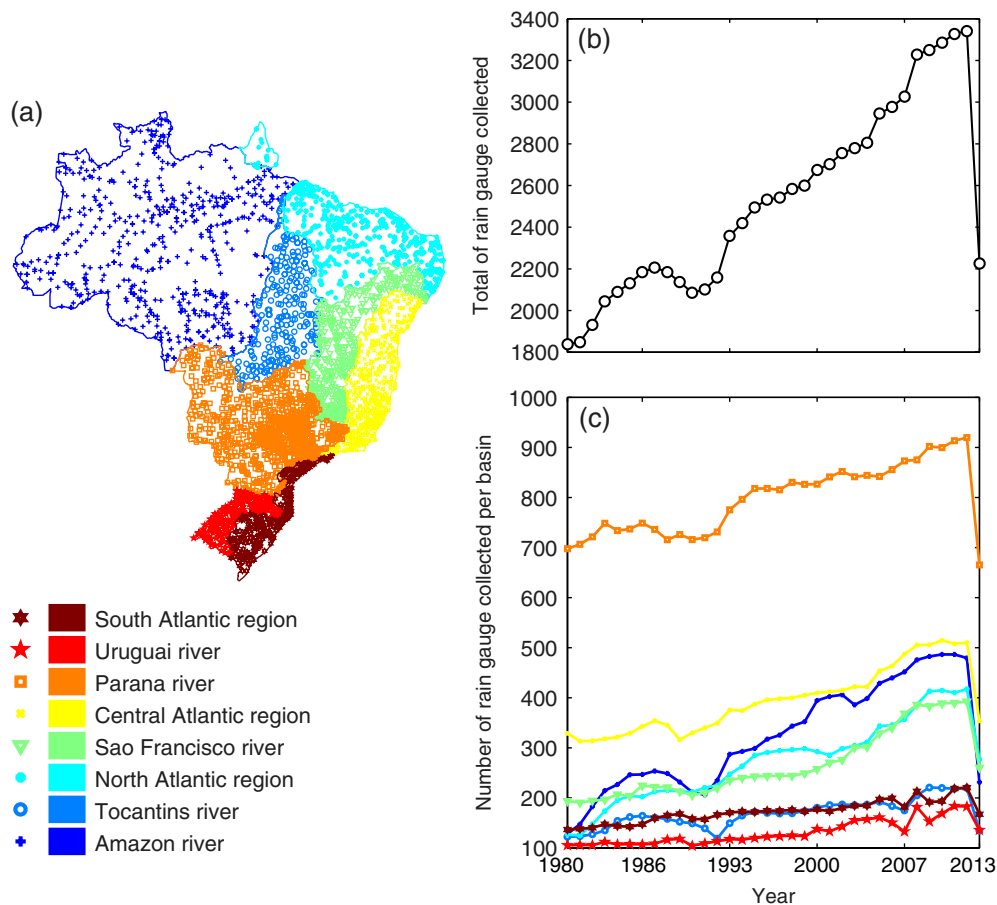


Figure 2. Major river basins of Brazil and spatial distribution of all rain gauges in the data set (a); the historical count of rain gauges in Brazil (b) and for each major river basin (c).

very high number of low and zero rainfall data, we tested *pr* only for CSI and CSIH (as per Hofstra *et al.* (2008)).

For each statistic used to determine the accuracy of the interpolation methods, we determine a ‘skill score’, that is the ranking of the interpolation method (1 = best, 2 = second best, etc.). The overall skill score for a given interpolation method is the average of the individual skill scores. For each meteorological variable, the best interpolation method is the one with the lowest (best) overall skill score.

Once we determined the best interpolation methodology for each variable (Section 3.2.1.), we show the results of cross validation: (1) at a daily timescale, considering Brazil (Section 3.2.3.); and (2) in the major river basins in Brazil, considering all time series (Section 3.2.4.). In Section 3.2.5., we show the results of gridded data sets that we generated.

3. Results

3.1. Spatial and temporal distribution of rain gauges and weather stations

The spatial distribution of all rain gauges in our data set and temporal variability in the average number of rain gauges available during the years analysed are shown throughout

Brazil and within the river basins (Figure 2(a), (b), and (c)). In 2012, the year with the highest number of available stations and data, the Amazon river basin has the lowest density of rain gauges, approximately 0.1 station per 1000 km², while the Atlantic (east and north/northeast basins), Parana, and Uruguai river basins have the highest density of gauges, approximately 1.0 per 1000 km². The average density of rain gauges for Brazil overall in 2012 was 0.4 stations per 1000 km². For comparison, the United States has approximately 1.1 stations per 1000 km² (NOAA, 2010). There is also a wide range in distribution of rain gauges within river basins. In the Amazon river basin, large areas have no weather stations, and subsequently our interpolations for *pr* are the least accurate and precise within the Amazon basin.

Throughout Brazil and within our data set, the total number of rain gauges with data generally increases from 1854 in 1980 to 3358 in 2012 before decreasing in 2013 (Figure 2(b) and (c)). We attribute the decline in 2013 to a time delay for government agencies to organize the data and make them available. We observe this same time delay for data from weather stations (see Figure 3(b)).

Similar to the spatial and temporal distribution of rain gauges, the Amazon river basin has the lowest density of weather stations (Figure 3(a)). The average number of available weather stations has generally increased at

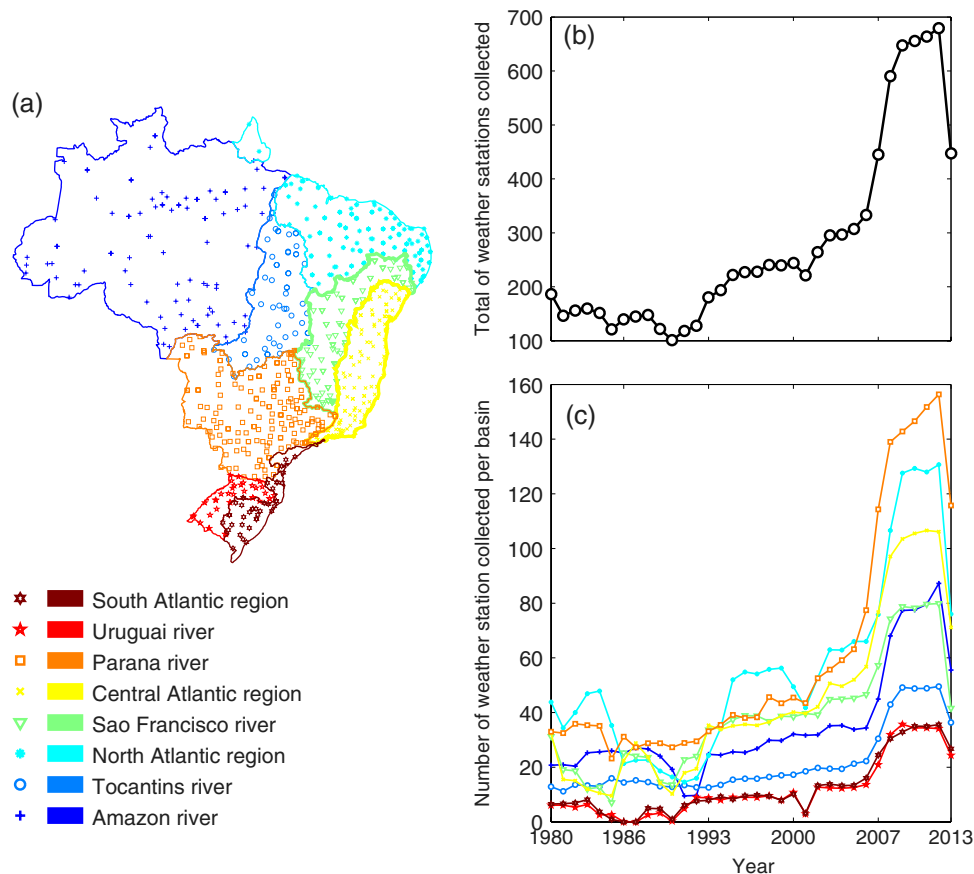


Figure 3. Major river basins of Brazil and spatial distribution of weather stations (a); annual average of the number of weather stations in Brazil (b) and for each major river basin (c).

a constant linear rate since 1980, with some downward fluctuations in the early 1990s (Figure 3(b) and (c)). For two river basins, the South Atlantic region and Uruguay river, there were no available weather station data for the years 1986, 1987, and 1990. Most of the weather stations installed before 2000 were of the ‘conventional’ variety and are mostly still functioning. After 2000, most installed stations are automatic.

3.2. Evaluating interpolation methods

3.2.1. Skill scores for all observed data

In interpolating each meteorological variable at a given rain gauge (for pr) or weather station, the most accurate interpolation method might differ for each variable. The gridded data sets (in multiple individual files grouped by variable type and time span) are available for download via a file sharing system of the University of Texas. Table 4 shows the statistics and their skill scores of the relationship between all daily observed and estimated data for pr and ETo (see Table S1, Supporting Information, for the other variables; direct link to data: <https://utexas.box.com/Xavier-et-al-IJOC-DATA>. Supplemental and README file: <https://utexas.box.com/Xavier-et-al-IJOC-SUPPLEMENTAL>. Author website with link to data and supplemental material: <http://careyking.com/data-downloads/>). For pr, the statistics were calculated

from approximately 32 million pairs of observed and estimated data per interpolation method. For the other meteorological variables and ETo, there are approximately 3.5 million pairs of data.

The best overall skill scores were generally obtained using ADW and IDW, where ADW was best for the variables ETo, R_s , RH, and u_2 and IDW for pr, T_{\min} , and T_{\max} . THINPLATE is almost as accurate as IDW and ADW in interpolating temperatures and solar radiation, R_s , as these variables change more smoothly over short distances. For pr, IDW and ADW are clearly superior to the other methods. THINPLATE, OPK, and NATURAL methods result in intermediate skill scores, and the AVERAGE interpolation method always has the worst skill score. We found a high correlation in the cross validation for ETo, T_{\max} , T_{\min} , R_s , and RH (R approximately 0.8–0.9) while much lower correlations exist for pr and u_2 (R approximately 0.4–0.6). All R values are statistically significant at p -value < 0.05 .

Biases are generally small for all variables and methods when we consider the magnitude of the variables. RMSE, CRE, and MAE are quite similar for all interpolation methods for a given variable, but ADW and IDW usually show better results (lower error statistics).

The ability of the interpolation methods to ‘forecast’ the state of pr, wet or dry, is moderately high (see PC

Table 4. Statistics and their respective skill score for pr and ETo.

Variables	Method	AV rank	R	#	Bias	#	RMSE	#	CRE	#	MAE	#	PC	#	CSI	#	CSIL	#	CSIH	#
pr	IDW	2.250	0.609	2	0.004	3	9.141	2	0.666	2	3.709	1	0.783	5	0.534	1	n/a	n/a	0.290	2
	ADW	2.375	0.621	1	0.003	2	8.889	1	0.630	1	3.713	2	0.771	6	0.525	5	n/a	n/a	0.292	1
	OPK	3.125	0.584	3	0.038	5	9.542	3	0.726	3	3.822	3	0.792	3	0.533	2	n/a	n/a	0.278	3
	NATURAL	3.875	0.563	5	0.001	1	9.871	5	0.777	5	3.891	4	0.797	2	0.528	4	n/a	n/a	0.270	5
	THINPLATE	4.250	0.577	4	0.145	6	9.656	4	0.743	4	3.911	5	0.788	4	0.529	3	n/a	n/a	0.272	4
	AVERAGE	5.125	0.511	6	-0.008	4	10.985	6	0.962	6	4.161	6	0.813	1	0.510	6	n/a	n/a	0.246	6
ETo	ADW	1.571	0.876	1	-0.004	5	0.775	1	0.234	1	0.575	1	n/a	n/a	n/a	n/a	0.548	1	0.389	1
	IDW	2.143	0.873	2	0.001	3	0.785	2	0.241	2	0.581	2	n/a	n/a	n/a	n/a	0.545	2	0.382	2
	OPK	2.714	0.869	3	0.001	1	0.800	3	0.249	3	0.589	3	n/a	n/a	n/a	n/a	0.542	3	0.377	3
	THINPLATE	3.714	0.863	4	0.001	2	0.817	4	0.261	4	0.601	4	n/a	n/a	n/a	n/a	0.534	4	0.369	4
	NATURAL	4.857	0.855	5	-0.001	4	0.844	5	0.278	5	0.619	5	n/a	n/a	n/a	n/a	0.518	5	0.359	5
	AVERAGE	6.000	0.824	6	-0.013	6	0.949	6	0.351	6	0.695	6	n/a	n/a	n/a	n/a	0.489	6	0.326	6

n/a, not applicable.

and CSI, Table 4). In the case of PC (the fraction of correctly interpolated days as 'wet' = $pr > 0.5 \text{ mm day}^{-1}$ and 'dry' otherwise), the AVERAGE method is most accurate at 81%, whereas ADW is the least accurate at 77%. We attribute AVERAGE providing the highest PC to the fact that it best represents the true spatial variability in precipitation. All of the other methods perform more smoothing of the data, effectively overestimating rainfall when there is none (e.g. 0 mm day^{-1}) and underestimating high precipitation events. This smoothing and underestimation of high precipitation days explains why CSIH is low (< 0.3) for all interpolation methods, with the better results obtained using ADW and IDW.

The interpolation results for u_2 are the least accurate overall as compared to the other meteorological variables. This finding is expected, as local geography can highly influence wind speed and gusts. CSIL and CSIH (observed and estimated values fall below/above the 5th/95th percentiles) are particularly low for u_2 , indicating similar difficulties for interpolating low wind speeds as for low precipitation. For the other variables, only low values are shown to be forecast with reasonable accuracy, slightly lower than those found in Hofstra *et al.* (2008).

The statistical values for our most accurate interpolation methods are generally slightly lower than those obtained by Hofstra *et al.* (2008) who interpolate weather over Europe, based on a much higher geographical density of weather stations. For example, Hofstra *et al.* (2008) obtain the following R values: 0.75 (global kriging), 0.98 (THINPLATE three dimension), and 0.96 (global kriging), for pr, T_{\max} , and T_{\min} , respectively. The highest R values for those same variables in our Brazil study are 0.62 (ADW for pr), 0.91 (IDW for T_{\max}), and 0.91 (IDW for T_{\min}).

3.2.2. Spatial distribution of the best models

The spatial distribution of the best interpolation method (best average skill score) for the rain gauges/weather stations for each meteorological variable is shown in Figure 4 for pr and ETo (see Figure S1 for the other variables). The two interpolation methods with the highest frequency (number of stations) of being the most accurate are ADW and IDW, where IDW is accurate most frequently for the

variables pr, T_{\max} , and T_{\min} , and ADW for ETo, RH, R_s , and u_2 . OPK, THINPLATE, and NATURAL methods show intermediate frequency of being the most accurate, and the AVERAGE interpolation is usually the least accurate. Interestingly, there does not appear to be any spatial or geographic pattern that explains why a given interpolation method is most accurate. Hofstra *et al.* (2008) found, for example, for the European stations that OPK method was the best for the pr, while NATURAL was the best for T_{\max} and T_{\min} . They also observed that in regions with dense station network and with less topographical complexity the local kriging (similar to OPK method, but with different variograms at each interpolation point) showed better results for pr.

3.2.3. Analysis of daily data

The daily statistical results of our cross-validation procedure are based on interpolating weather variables at the location of each station at daily time resolution. Figure 5 shows an example of calculating the statistical metrics for a single day, 1 January 1980. We show two variables: pr and ETo. If the interpolation estimate is perfect, then all data points would lie on the line with a slope 1 (1 : 1 line). Across Brazil for this single day, there are 1854 rain gauges and 135 weather stations with available data. Thus, there are 1854 and 135 pairs of observed and estimated data for pr and ETo, respectively, for the cross-validation procedure. We estimated pr and ETo using IDW and ADW interpolations, respectively, as described previously (Table 4). For pr on 1 January 1980, for example, R is 0.71, RMSE is 11.0 mm, and bias is -0.05 mm (Figure 5(a)). Other statistics for that day can be observed in the Figure 5(a) and (b).

We repeated this cross-validation procedure for every day, and we summarize the results for pr and ETo in Figures 6 and 7, and for the other variables, Figures S2–S6. The results in Table 4 are the summarized skill scores averaged from all days. Both Figures 6 and 7 follow the same format for displaying the individual daily calculations. For the upper scatter plot for each skill score, rows indicate the years (1980–2013) and columns indicate the days (1 January to 31 December) for the calculation. The

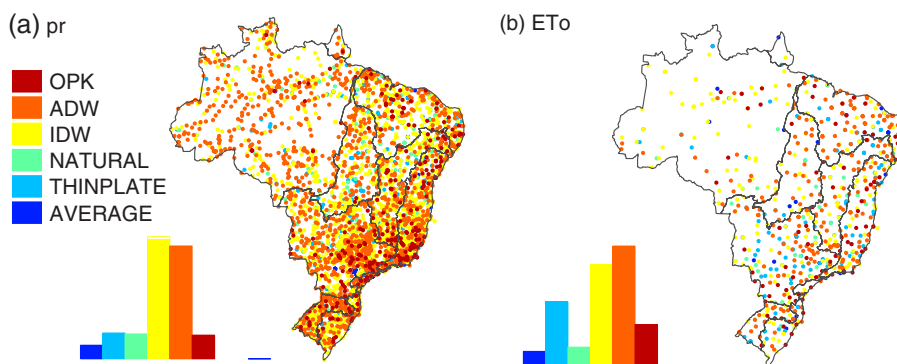


Figure 4. The most precise interpolation method, as measured by highest average skill score, is indicated for Brazil overall (relative frequency histogram in lower left of each plot) and for each station (coloured dots on the map) for both pr (a) and ETo (b). Each interpolation method from top to bottom in the legend is represented from right to left in the histograms.

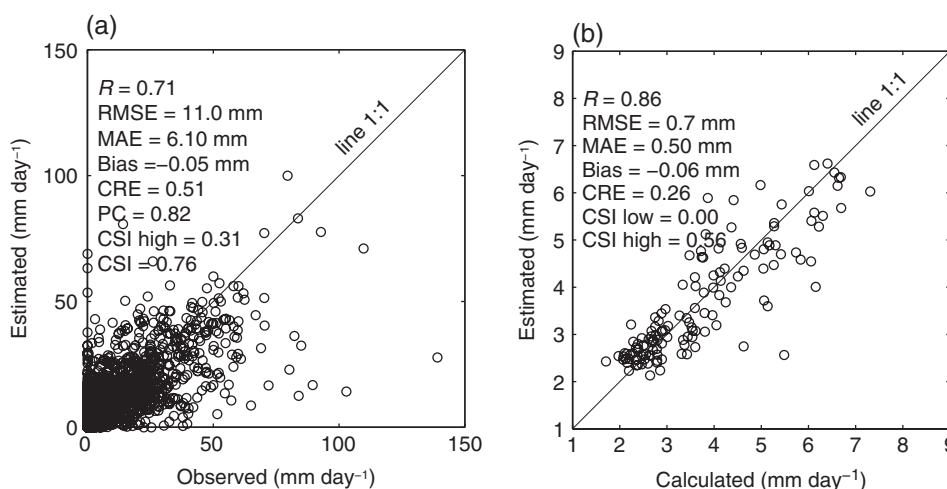


Figure 5. Scatter diagram of estimated versus observed pr (a) and ETo (b) using, respectively, IDW and ADW method for 1 January 1980. Each plot shows the individual skill scores for that single day.

colour bar indicates the skill score for each daily calculation. Below each coloured scatter plot is a line plot indicating the average skill score across each year for a given day. The value of this line plot is to assess whether certain times of the year are more accurately estimated than others. For example, Figure 6 shows that for RMSE is much lower, and PC is much higher, when interpolating precipitation during the winter months (July and August).

3.2.3.1. *Precipitation:* Figure 6 presents our interpolation results and skill scores using the IDW interpolation method. Daily R and bias (Figure 6(a) and (b)) do not indicate a clear seasonal trend between them, except for perhaps higher R in the winter season. The daily averages are approximately constant at $R=0.50$ and bias approximately 0.00 mm. RMSE is much lower, and PC is much higher during the winter months (July and August) indicating that precipitation is more easily predictable in the winter due to lower precipitation as compared to spring and summer (see Figure 6(d)). In the dry seasons (fall and winter), the forecast of the state of precipitation (PC) and the 95th percentile (CSIH) are both more accurate. CRE seems to show higher accuracy in fall and early winter, but with greater uncertainty.

3.2.3.2. *Evapotranspiration:* The skill scores for ETo, Figure 7, are based on comparing ETo calculated using observed input from the weather station to ETo calculated using interpolated data for that same weather station. Most of the skill scores are relatively uniform for all days throughout the year. RMSE is lowest during the fall (April and May) and highest during the spring. A few of the skill scores are poor for 1990 because of a relatively high quantity of missing data from weather stations.

3.2.3.3. *Temperature:* The behaviour of T_{max} and T_{min} is similar (Figures S2 and S3) except for one metric. T_{min} shows a clear increase in RMSE in the winter months that is not present in T_{max} . For T_{max} and T_{min} , between 1980 and 2005, the daily R , mainly in summer is lower than during the fall and winter. After 2005, R is much higher throughout the year. We attribute this anomalous trend to the higher number of missing data in the data set during that period (1980–2005) and less variation in temperature over all Brazil in that season. The autumn and winter seasons have high temperature variations in Brazil, with low temperature in the south region and high in the north of Brazil. Thus, there is an increased possibility of higher R in the cross validation across all of Brazil for autumn

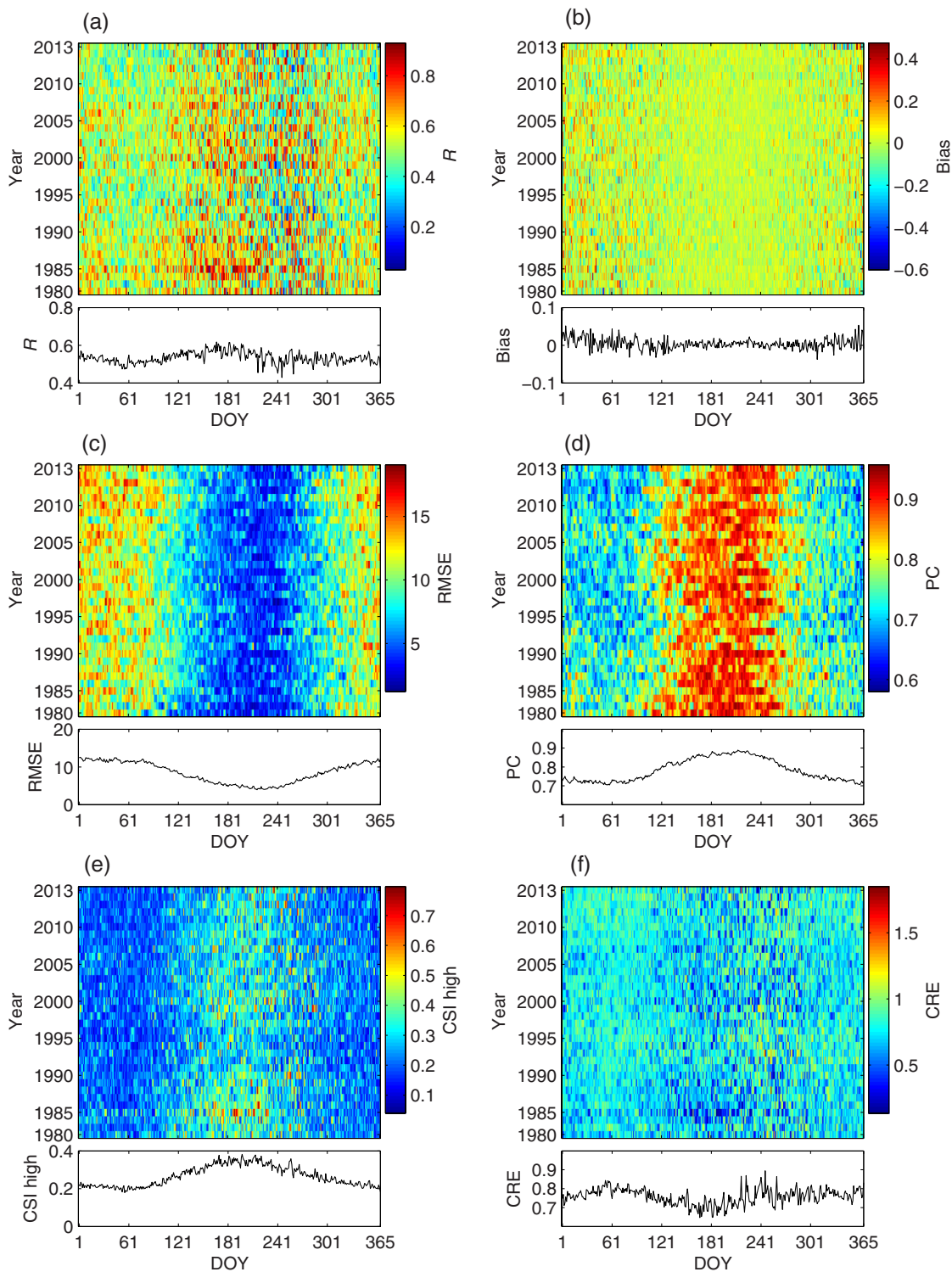


Figure 6. Daily skill scores of the relationship between observed and estimated pr when interpolating using IDW.

and winter. The forecast (CSI low, CSIL, and high, CSIH) is greater in the recent years (2005–2013). This trend is due to the increase in number of weather stations such that there is increased power for interpolating the data.

3.2.3.4. Solar radiation: As with precipitation, R_s has higher interpolation accuracy (e.g. lower RMSE, higher CSI low, see Figure S4) during the winter than summer

months, likely due to less variability in cloud cover and lower radiation magnitude. A few of the skill scores (R and CRE) are poor from 1990 to 1995 due to a relatively high quantity of missing data from weather stations.

3.2.3.5. Relative humidity: For interpolating RH (Figure S5), there is both highest R and RMSE in the late winter and early spring. During that time of the year, many regions

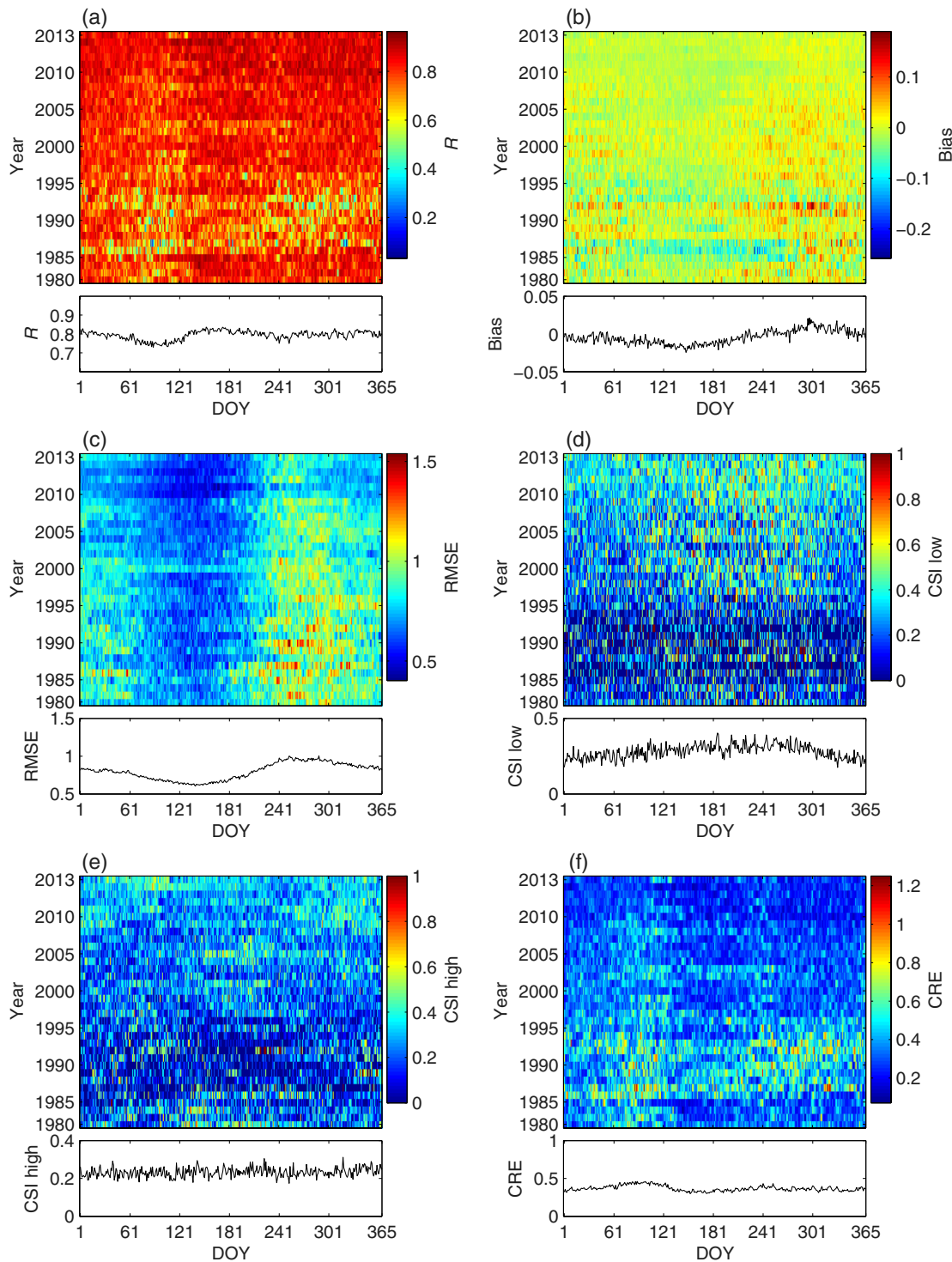


Figure 7. Daily skill scores of the relationship between ETo calculated using observed data versus estimated data when interpolating using ADW.

in Brazil are dry, but the Amazon region still has high RH. Thus, there are some places with consistently low RH and some with consistently high RH, and both situations promote a high R metric for RH during late winter and early spring. This increased RMSE during this time is mostly present in the data before 2005, and correlation, R , is highest after 2005 during the spring. These trends for R and RMSE might be driven by peculiar aspects related to data collection via conventional weather stations

dominating pre-2005 data and automatic stations after 2005. It is also possible that the increased accuracy of measurement post-2005 is due to simply having a higher number of active weather stations. A few of the skill scores (R , bias, and CRE) are poor before 1995 due to a relatively high quantity of missing data from weather stations.

3.2.3.6. *Wind speed:* Generally, the skill scores are poor for interpolating u_2 (Figure S6). Correlation is less than

Table 5. Cross-validation results for interpolation methods per variable and per basin.

Variables (methods)	Basin	<i>R</i>	Bias	RMSE	CRE	MAE	PC	CSI	CSIL	CSIH
pr (IDW)	Amazon river	0.362	-0.007	13.069	0.982	6.794	0.636	0.481	n/a	0.132
	Tocantins river	0.503	-0.013	10.544	0.803	4.639	0.750	0.498	n/a	0.200
	North Atlantic region	0.577	0.020	9.242	0.715	3.725	0.776	0.524	n/a	0.262
	Sao Francisco river	0.699	0.013	6.832	0.532	2.322	0.858	0.562	n/a	0.376
	Central Atlantic region	0.669	0.040	7.410	0.575	2.803	0.797	0.540	n/a	0.352
	Parana river	0.655	0.000	8.401	0.597	3.287	0.812	0.554	n/a	0.328
	Uruguay river	0.724	0.017	9.087	0.490	3.532	0.807	0.546	n/a	0.407
	South Atlantic region	0.720	-0.094	8.488	0.497	3.286	0.804	0.591	n/a	0.395
ETo (ADW)	Amazon river	0.703	0.014	0.804	0.528	0.609	n/a	n/a	0.289	0.164
	Tocantins river	0.776	-0.003	0.764	0.404	0.578	n/a	n/a	0.370	0.303
	North Atlantic region	0.840	0.034	0.893	0.296	0.672	n/a	n/a	0.383	0.316
	Sao Francisco river	0.868	-0.092	0.804	0.250	0.606	n/a	n/a	0.408	0.346
	Central Atlantic region	0.872	0.035	0.738	0.241	0.548	n/a	n/a	0.389	0.312
	Parana river	0.873	-0.006	0.709	0.238	0.524	n/a	n/a	0.536	0.349
	Uruguay river	0.937	-0.012	0.625	0.122	0.453	n/a	n/a	0.506	0.445
	South Atlantic region	0.931	0.023	0.603	0.133	0.438	n/a	n/a	0.480	0.429

n/a, not applicable.

$R = 0.6$ over the course of the year, and the interpolation method has a slight downward bias. A few of the skill scores (R , bias, and CRE) are exceptionally poor before 1995 due to a relatively high quantity of missing data from weather stations. For some stations, we calculated negative R because of so much missing data. Overall, estimation of wind speed is expected to be poor because of localized effects, including elevation factors that were not included in our analysis.

3.2.4. Interpolation results for river basins

To evaluate spatial variations in meteorological parameters across Brazil, we calculated cross-validation skill score statistics for major river basins in Brazil (see Table 5). We used the interpolation method with the best overall skill score for each variable as discussed in Section 3.2. Skill score statistics are poorest for the Amazon River basin for all variables because of the low number and density of available weather stations. Basins with a greater number of stations and station density provide much better results. Basins with high station density are the Parana, Uruguay, South Atlantic region, and São Francisco basins.

It is useful to compare results in Table 5 to those in Table 4. For example, for pr, we use IDW that has $R = 0.61$ and $PC = 0.78$ for Brazil overall (Table 4). Comparing results from the river basins with those for Brazil overall shows that five river basins have higher R and PC , one is equal to and two (Amazon and Tocantins) are less than each metric for Brazil overall. As another example, consider ETo using ADW which results in $R = 0.88$ and $RMSE = 0.78$ for Brazil overall (Table 4). Two of the river basins have R greater than, three approximately equal, and three lower than R for overall Brazil. For RMSE of interpolating ETo, one river basin (North Atlantic region) has greater, six have approximately equal, and two have less than the RMSE for overall Brazil.

3.2.5. Gridded data sets

Using the interpolation method with the best skill score for each weather variable, we created gridded daily and monthly weather data across Brazil at $0.25^\circ \times 0.25^\circ$ spatial resolution. The data are in Network Common Data Form (NetCDF) that includes grid coordinates, dates, and other relevant information. They are available online see: <http://careyking.com/data-downloads>.

Our grid coordinates coincide with those in the TRMM data set. Thus, our data complement TRMM data that are available since 1998. For instance, it is possible to compare our gridded station-based precipitation to estimated precipitation in TRMM. We also include two indicators of the quality of each grid cell: the number of included stations with data, and the geodesic distance of the nearest reporting station with data.

Figure 8 compares observed pr (left) at each station with our interpolated gridded data (right) for two days, 1 December 1980 and 1 December 2010. These two days have 1869 and 3390 rain gauges, respectively. In this example, we observe that large areas, for example in the Amazon river basin, with few rain gauges cause large areas to have similar pr estimates in the gridded data. As the number of rain gauges increased through 2010, the gridded data in turn were able to provide higher resolution. This same pattern toward higher resolution is observed for the other weather variables (e.g. see Figure 9 displaying ETo calculated at weather stations *versus* calculated using interpolated gridded data). To generate gridded ETo data, we calculate ETo only at weather stations that have all the necessary data at the weather station for a particular day, and then interpolate these ETo from the weather stations to the grid. We do not first interpolate the underlying individual weather data for ETo to a grid and then estimate ETo from those gridded interpolations.

Oftentimes researchers and planners use models with monthly data instead of daily data. Thus, we provide data at both daily and monthly time steps to facilitate different

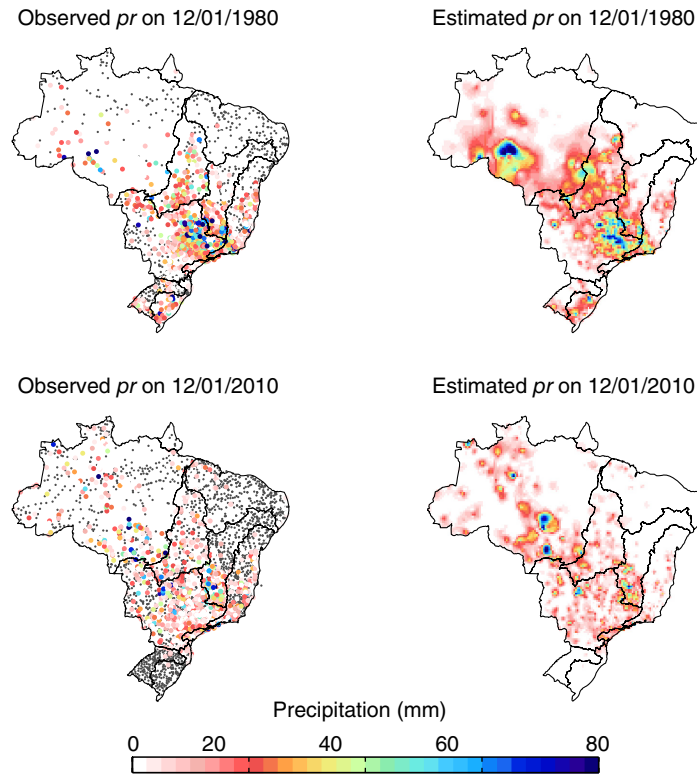


Figure 8. Scatter diagram of observed pr and its respective gridded map in two dates, 1 December 1980 and 1 December 2010. Grey dots points are rain gauges or weather stations with pr = 0 mm on the respective day.

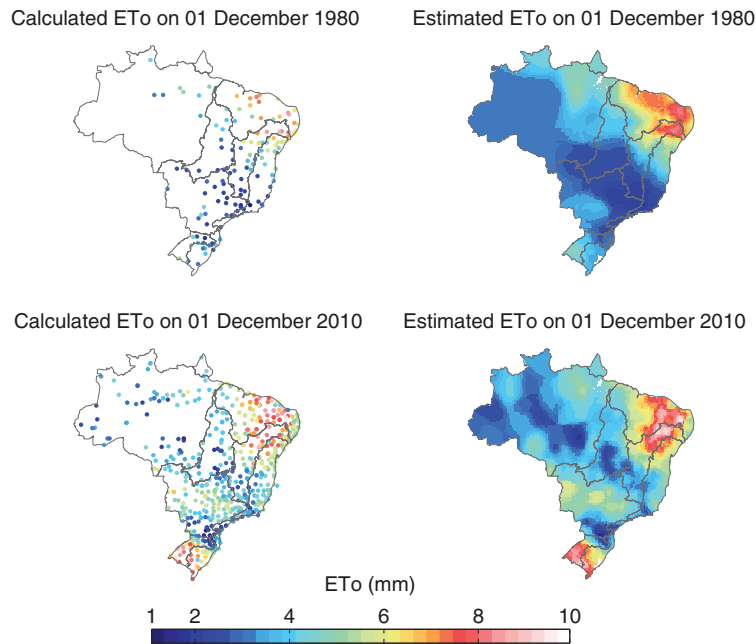


Figure 9. Scatter diagram of calculated ETo using observed data and its respective gridded map on two dates, 1 December 1980 and 1 December 2010.

models. For example, the decision support systems for agrotechnology transfer (Jones *et al.*, 2003, DSSAT) models use daily inputs, and CROPWAT (Smith, 1992) can use monthly or daily inputs. Figures S7 and S8 show the monthly average pr and ETo, respectively, for the period of 1980–2013 in Brazil. One can see the low pr in the São Francisco river basin as half of the year has

monthly precipitation of less than 20 mm. Further, this basin has relatively large values of ETo, suggesting that, without irrigation, water could be a limiting factor for crop yields. These monthly data can be used for broad planning purposes such as agroecological and crop zoning and drought analysis (e.g. Rubel and Kotteck, 2010; Jabot *et al.*, 2012; Assad *et al.*, 2013; Cook *et al.*, 2014).

4. Conclusions

We studied the potential of six different interpolation methods to estimate six weather variables (T_{\min} , T_{\max} , RH, R_s , u_2 , and pr) and reference ET, ETo. We obtained the weather data from 3625 rain gauges and 735 weather stations that recorded data any time from 1980 through 2013. Using cross-validation analysis, we determined that IDW or ADW were the best interpolation methods for all variables.

We found that performance depends on both the amount of data available and the season. For example, generally, the performance of the interpolations is better in recent years due to the increased number of weather stations. Because of lower precipitation levels during autumn and winter, the interpolations for precipitation are more accurate during those seasons. The forecast of extreme high or low values for weather variables is always weak (< 65%), and wind speed (u_2) has the lowest interpolation accuracy of all weather variables.

Skill scores for meteorological variables are lower (with more accurate interpolation) for river basins with higher gauge or station densities (e.g. Uruguay River, Central and South Atlantic regions). In contrast, the Amazon River, with the lowest data density, has the worst skill scores for all variables studied.

Daily and monthly gridded data were generated for the variables, at a resolution of $0.25^\circ \times 0.25^\circ$. Development of daily and monthly gridded weather data for Brazil will significantly advance our ability to assess the reliability of satellite-based products and to evaluate the impacts of climate variability on water resources and crop production.

Acknowledgements

This project is part of the International Climate Initiative (IKI). The German Federal Ministry for the Environment, Nature Conservation, Building and Nuclear Safety (BMUB) supports this initiative on the basis of a decision adopted by the German Bundestag. The project number is 12_II_100_BRA_A_COPPETEC. The authors declare no conflicts of interest.

Supporting Information

The following supporting information is available as part of the online article:

Appendix S1. Additional data in tables and figures as well as instructions for downloading and using the gridded meteorological data set described in this manuscript. The data are free for use. The link to the data is available via the corresponding author's website, <http://careyking.com/data-download/>.

References

Allen RG, Pereira DR, Raes D, Smith M. 1998. *Crop Evapotranspiration: Guidelines for Computing Crop Water Requirements*, 1st edn. United Nations, FAO: Rome. <http://www.kimberly.uidaho.edu/ref-et/fao56.pdf> (accessed 1 July 2014).

- Assad ED, Martins SC, Beltrao NEdM, Pinto HS. 2013. Impacts of climate change on the agricultural zoning of climate risk for cotton cultivation in Brazil. *Pesq. Agropec. Bras.* **48**: 1–8.
- Bruinsma J. 2003. World agriculture: towards 2015–30, an FAO perspective, Technical Report, FAO and Earthscan, Rome and London.
- Cook BI, Seager R, Smerdon JE. 2014. The worst North American drought year of the last millennium: 1934. *Geophys. Res. Lett.* **41**(20): 7298–7305, doi: 10.1002/2014GL061661.
- Daly C, Halbleib M, Smith JI, Gibson WP, Doggett MK, Taylor GH, Curtis J, Pasteris PP. 2008. Physiographically sensitive mapping of climatological temperature and precipitation across the conterminous United States. *Int. J. Climatol.* **28**(15): 2031–2064, doi: 10.1002/joc.1688.
- FAOSTAT. 2014. Website of the Food and Agriculture Organization of the United Nations - Statistics Division. <http://faostat.fao.org/site/339/default.aspx> (accessed 1 July 2014).
- Harris I, Jones P, Osborn T, Lister D. 2014. Updated high-resolution grids of monthly climatic observations – the CRU TS3.10 dataset. *Int. J. Climatol.* **34**(3): 623–642, doi: 10.1002/joc.3711.
- Haylock MR, Peterson TC, Alves LM, Ambrizzi T, Anunciação YMT, Baez J, Barros VR, Berlato MA, Bidegain M, Coronel G, Corradi V, Garcia VJ, Grimm AM, Karoly D, Marengo JA, Marino MB, Moncunill DF, Nechet D, Quintana J, Rebello E, Rusticucci M, Santos JL, Trebejo I, Vincen LA. 2006. Trends in total and extreme South American rainfall in 1960–2000 and links with sea surface temperature. *J. Clim.* **19**: 1490–1512.
- Haylock MR, Hofstra N, Klein Tank AMG, Klok EJ, Jones PD, New M. 2008. A European daily high-resolution gridded data set of surface temperature and precipitation for 1950–2006. *J. Geophys. Res. Atmos.* **113**(D20): 1–12, doi: 10.1029/2008JD010201.
- Hofstra N, New M. 2009. Spatial variability in correlation decay distance and influence on angular-distance weighting interpolation of daily precipitation over Europe. *Int. J. Climatol.* **29**(12): 1872–1880, doi: 10.1002/joc.1819.
- Hofstra N, Haylock M, New M, Jones P, Frei C. 2008. Comparison of six methods for the interpolation of daily, European climate data. *J. Geophys. Res. Atmos.* **113**(D21): 1–19, doi: 10.1029/2008JD010100.
- Huffman GJ, Adler RF, Morrissey MM, Bolvin DT, Curtis S, Joyce R, McGavock B, Susskind J. 2001. Global precipitation at one-degree daily resolution from multisatellite observations. *J. Hydrometeorol.* **2**: 36–50.
- Huffman GJ, Bolvin DT, Nelkin EJ, Wolff DB, Adler RF, Gu G, Hong Y, Bowman KP, Stocker EFDB. 2007. The TRMM multisatellite precipitation analysis (TMPA): quasi-global, multiyear, combined-sensor precipitation estimates at fine scales. *J. Hydrometeorol.* **8**: 38–55.
- ICONE. 2012. Outlook Brazil 2022: Agribusiness projections, Technical Report, FIESP and ICONE, São Paulo.
- Jabot E, Zin I, Lebel T, Gautheron A, Obed C. 2012. Spatial interpolation of sub-daily air temperatures for snow and hydrologic applications in mesoscale alpine catchments. *Hydrol. Process.* **26**(17): 2618–2630, doi: 10.1002/hyp.9423.
- Jones J, Hoogenboom G, Porter C, Boote K, Batchelor W, Hunt L, Wilkens P, Singh U, Gijsman A, Ritchie J. 2003. DSSAT cropping system model. *Eur. J. Agron.* **18**: 235–265.
- Jung M. 2009. Towards global empirical upscaling of FLUXNET eddy covariance observations: validation of a model tree ensemble approach using a biosphere model. *Biogeosciences* **6**(10): 2001–2013.
- Karaseva M, Prakash S, Gairola R. 2012. Validation of high-resolution TRMM-3B43 precipitation product using rain gauge measurements over Kyrgyzstan. *Theor. Appl. Climatol.* **108**(1–2): 147–157, doi: 10.1007/s00704-011-0509-6.
- Li X-H, Zhang Q, Xu C-Y. 2012. Suitability of the TRMM satellite rainfalls in driving a distributed hydrological model for water balance computations in Xinjiang catchment, Poyang Lake basin. *J. Hydrol.* **426–427**: 28–38.
- Liebmann B, Allured D. 2005. Daily precipitation grids for South America. *Bull. Am. Meteorol. Soc.* **86**: 1567–1570. http://www.esrl.noaa.gov/psd/data/gridded/data.south_america_precip.html (accessed 28 May 2015).
- Ly S, Charles C, Degré A. 2011. Geostatistical interpolation of daily rainfall at catchment scale: the use of several variogram models in the Ourthe and Ambleve catchments, Belgium. *Hydrol. Earth Syst. Sci.* **15**(7): 2259–2274.
- Moradi I. 2009. Quality control of global solar radiation using sunshine duration hours. *Energy* **34**(1): 1–6.
- Mu Q, Zhao M, Running SW. 2011. Improvements to a MODIS global terrestrial evapotranspiration algorithm. *Remote Sens. Environ.* **115**(8): 1781–1800.

- New M, Hulme M, Jones P. 2000. Representing twentieth-century space-time climate variability. Part II: development of 1901–96 monthly grids of terrestrial surface climate. *J. Clim.* **13**: 2217–2238.
- New M, Lister D, Hulme M, Makin I. 2002. A high-resolution data set of surface climate over global land areas. *Clim. Res.* **21**: 1–25.
- NOAA. 2010. NOAA partnerships: cooperative observer program, Technical Report, National Oceanic and Atmospheric Administration, Silver Spring, MD.
- Peterson TC, Easterling DR, Karl TR, Groisman P, Nicholls N, Plummer N, Torok S, Auer I, Boehm R, Gullett D, Vincent L, Heino R, Tuomenvirta H, Mestre O, Szentimrey T, Salinger J, Forland EJ, Hanssen-Bauer I, Alexandersson H, Jones P, Parker D. 1998. Homogeneity adjustments of in situ atmospheric climate data: a review. *Int. J. Climatol.* **18**(13): 1493–1517, doi: 10.1002/(SICI)1097-0088(19981115)18:13<1493::AID-JOC329>3.0.CO;2-T.
- Raes. 2012. *The ETo Calculator*. Food and Agriculture Organization of the United Nations, FAO: Rome.
- Rodell M, Houser PR, Jambor U, Gottschalk J, Mitchell K, Meng C-J, Arsenault K, Cosgrove B, Radakovich J, Bosilovich M, Entin JK, Walker JP, Lohmann D, Toll D. 2004. The Global Land Data Assimilation System. *Bull. Am. Meteorol. Soc.* **85**(3): 381–394.
- Rubel F, Kotteck M. 2010. Observed and projected climate shifts 1901–2100 depicted by world maps of the Köppen-Geiger climate classification. *Meteorol. Zeitschr.* **19**(2): 135–141.
- Shafer M, Fiebrich C, Arndt D, Fredrickson S, Hughes T. 2000. Quality assurance procedures in the Oklahoma mesonet. *J. Atmos. Ocean. Technol.* **17**: 474–494.
- Sibson R. 1981. A brief description of natural neighbor interpolation. In *Interpreting Multivariate Data*, Barnett V (ed). John Wiley and Sons: Chichester, UK, 21–36.
- Smith M. 1992. *CROPWAT: A Computer Program for Irrigation Planning and Management*, FAO Irrigation and Drainage Paper No. 46. Food and Agriculture Organization of the United Nations: Rome.
- Steduto P, Hsiao TC, Raes D, Fereres E. 2009. Aquacrop – the FAO crop model to simulate yield response to water: I. concepts and underlying principles. *Agron. J.* **101**: 426–437.
- Tao F, Zhang Z, Xiao D, Zhang S, Rotter RP, Shi W, Liu Y, Wang M, Liu F, Zhang H. 2014. Responses of wheat growth and yield to climate change in different climate zones of China, 198–2009. *Agric. For. Meteorol.* **189–190**: 9–104.
- Vincent LA, Peterson TC, Barros VR, Marino MB, Rusticucci M, Carrasco G, Ramirez E, Alves LM, Ambrizzi T, Berlato MA, Grimm AM, Marengo JA, Molion L, Moncunill DF, Rebello E, Anunciação YMT, Quintana J, Santos JL, Baez J, Coronel G, Garcia J, Trebejo I, Bidegain M, Haylock MR, Karoly D. 2005. Observed trends in indices of daily temperature extremes in South America 1960–2000. *J. Clim.* **18**: 5011–5023.
- Webster R, Oliver MA. 2007. *Geostatistics for Environmental Scientists*, 2nd edn. John Wiley & Sons: Chichester, UK.
- Wijngaard JB, Klein Tank AMG, Können GP. 2003. Homogeneity of 20th century European daily temperature and precipitation series. *Int. J. Climatol.* **23**(6): 679–692, doi: 10.1002/joc.906.
- Wilks DS. 2011. *Statistical Methods in the Atmospheric Sciences*, 3rd edn. Academic Press: Oxford, UK and Waltham, MA.
- Wu W, Xu A-D, Liu H-B. 2014. High-resolution spatial databases of monthly climate variables (1961–2010) over a complex terrain region in southwestern China. *Theor. Appl. Climatol.* **119**: 1–10, doi: 10.1007/s00704-014-1123-1.
- Xia Y, Fabian P, Winterhalter M, Zhao M. 2001. Forest climatology: estimation and use of daily climatological data for Bavaria, Germany. *Agric. For. Meteorol.* **106**(2): 87–103.
- You J, Hubbard KG, Nadarajah S, Kunkel KE. 2007. Performance of quality assurance procedures on daily precipitation. *J. Atmos. Oceanic Technol.* **24**: 821–834.
- Zhang K, Kimball JS, Nemani RR, Running SW. 2010. A continuous satellite-derived global record of land surface evapotranspiration from 1983 to 2006. *Water Resour. Res.* **46**: W09522, doi: 10.1029/2009WR008800.